

THE MAJOR CAUSE FOR SLIDING FAILURE OF SIDE WALLS DURING BASEMENT EXCAVATION IN HIGH-RISE BUILDINGS

Tse-Shan Hsu

Honorary President, Institute of Mitigation for Earthquake Shear Banding Disasters
Professor, Feng-Chia University, Taichung, Taiwan, R.O.C., tshsu@fcu.edu.tw

Lin-Yao Wang

Ph.D. and Director, Bureau of Transportation and Public Works, Yunlin, Taiwan, R.O.C.

Abstract

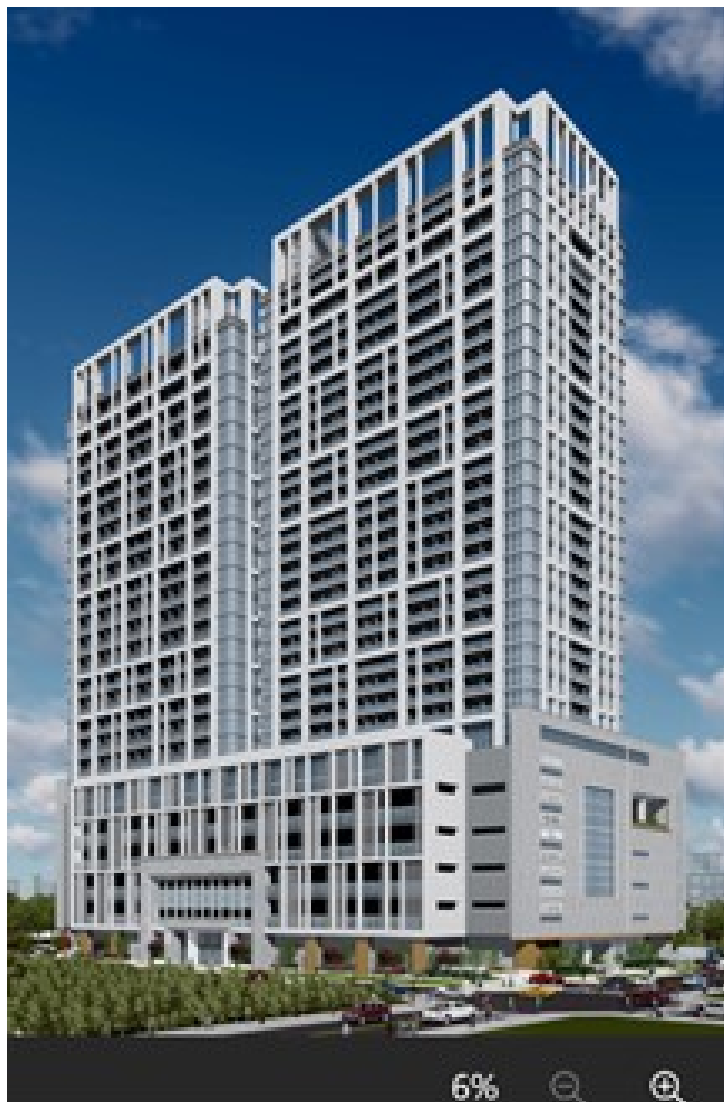
Despite the high shear strength of the strata in Zhubei, Taiwan, repeated side wall sliding failures have been observed during basement excavations for some high-rise buildings. This study uses the Fengcai-520 high-rise basement excavation as a case study to explore the underlying causes of sliding failures by comparing the results obtained from traditional design methods with those from performance-based design approaches. The results of this study reveal the following three conclusions: (1) Both design approaches encounter side wall sliding failures during excavation; (2) Increased shear banding during seismic events leads to greater brittleness of rock within shear bands, and resulting in highly concentrated excess pore water pressures in shear bands. This can cause rock debris to float, creating interconnected drainage pathways that direct water inflow into the basement; (3) Performance-based design is more effective than traditional methods. It swiftly addresses side wall sliding failures by dissipating concentrated excess pore water pressures, thus preventing further impacts on reinforced concrete side walls and ensuring the structural safety of the building. It is recommended that future basement excavations adopt performance-based design to reduce construction costs and enable rapid emergency responses, thereby ensuring the structural safety of the completed building.

Keywords: shear bands, basement excavation, sliding failure, performance-based design, traditional design.

Introduction

Stability design for side walls during basement excavation in high-rise buildings commonly employs two primary approaches: traditional design (McCarthy, 2007) and performance-based design (Simonelh and Penna, 2009). This study examines the excavation retaining structures of the six-story

basement and 32-story above-ground Fongcai-520 high-rise building in Zhubei, Taiwan (Figure 1). Traditional design methods necessitate the selection of safety factors as per regulations. These safety factors are used to determine the dimensions and penetration depth of H-shaped steel sections based on limit equilibrium analysis.



(a) North-facing perspective view.



(b) South-facing perspective view



Note: The length of the northern side is 164 meters, the southern side is 133 meters, the eastern side is 106 meters, and the western side is 97 meters.

(c) Site area (Google Earth, 2024).

Figure 1. Perspective views and site area of the Fengcai-520 high-rise in Zhubei, Taiwan.

Traditional design specifications rely on the Coulomb earth pressure formula, which is based on simplifying assumptions that may not accurately reflect complex soil conditions. Coulomb's model assumes a stable elastic-perfectly plastic behavior, whereas actual soil behavior is often unstable with strain-softening characteristics.

Research by Hsu, et al. (2021) indicates that Coulomb's formula, derived under stable conditions, does not induce a failure surface in the soil behind retaining walls. In contrast, an unstable plastic strain-softening model would better represent the actual failure conditions.

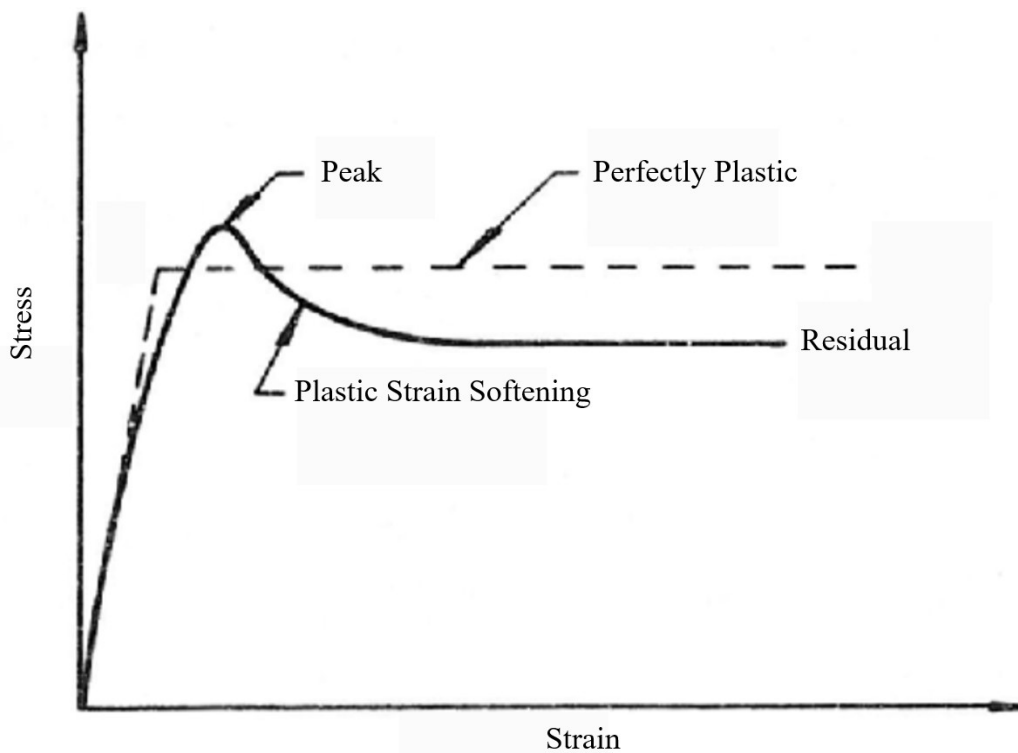


Figure 2. Comparison of the stress-strain relationship curves between actual soil and simplified soil (Chen, 1975).

Hsu, et al. (2021) demonstrated that under both active and passive earth pressure conditions, employing a stable perfectly plastic model does not accurately generate a failure surface within the soil behind a retaining wall. It is only with the use of an unstable plastic strain-softening model that a failure

surface is induced in the soil behind the retaining wall.

Consequently, when deriving formulas for active or passive earth pressures, Coulomb utilized a stable perfectly plastic model while simultaneously assuming the presence of an

unstable failure surface (McCarthy, 2009). This creates a fundamental incompatibility in Coulomb's earth pressure formula, as it relies on two mutually exclusive assumptions.

Engineers should be aware that the Coulomb earth pressure formula, as specified by design codes (National Land Management Agency, Ministry of the Interior, 2023), can lead to significant discrepancies between calculated and actual earth pressures on retaining walls. For example, in the case

of active earth pressure, the Coulomb formula has been shown to cause a substantial overestimation—by a factor of 2.5—due to its reliance on the stable perfectly plastic model rather than the unstable strain-softening model (Hsu, et al, 2021). As a result, retaining walls designed using this formula may be prone to failure under a variety of conditions, including during typhoons, heavy rainfall, earthquakes, or even under calm, dry conditions (see Figure 3).



(a) During heavy rainfall (New Taipei City, Taiwan; Hsu et al., 2021)



(b) During the 921 Jiji Earthquake (Taichung, Taiwan; Hsu et al., 2021)



(c) In the absence of wind, rain, and earthquakes (Keelung, Taiwan; Hsu et al., 2021).

Figure 3. Failure of retaining walls under various conditions.

Due to the inherent incompatibilities in the derivation of earth pressure formulas, retaining walls designed using conventional methods are susceptible to failure. In traditional retaining wall design, when in-situ stress conditions surpass the limit state and result in wall failure, the design outputs often fall short in addressing the extent of the failure, the residual functionality of the wall post-failure, and the acceptable level of wall damage.

These limitations of traditional design approaches lead to various unresolved issues. To address these challenges, performance-based design methodologies for retaining walls have been developed. This approach aims to overcome the shortcomings of conventional designs by offering solutions that better account for the real-world performance and resilience of retaining walls under diverse conditions.

Traditional and Performance-Based Design for the Retaining Structures of the Fengcai-520 High-Rise Basement Excavation

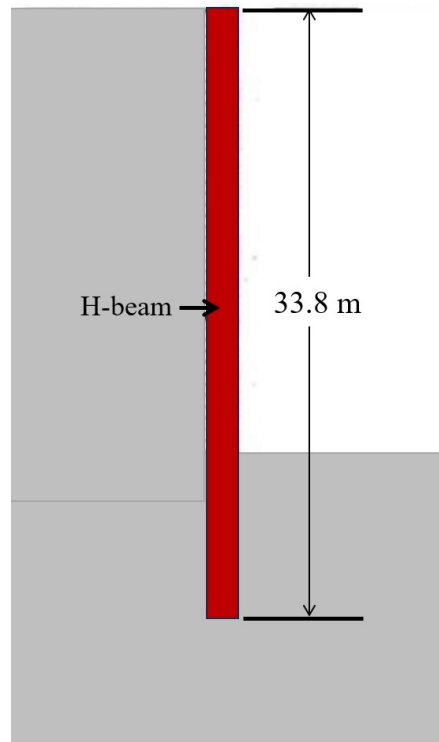
Traditional Design

In traditional design for retaining structures, the required safety factors under long-term loading conditions are as follows: the factor of safety against sliding should exceed 1.5, the factor of safety against overturning should be greater than 2.0, the factor of safety for

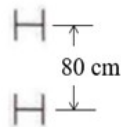
foundation bearing capacity should be greater than 3.0, and the overall stability factor should be more than 1.5. Under seismic loading conditions, the required safety factors are: a factor of safety against sliding greater than 1.2, a factor of safety against overturning greater than 1.5, a factor of safety for foundation bearing capacity greater than 1.2, and an overall stability factor greater than 1.1.

In practice, after selecting the safety factors according to regulations, engineers conduct equilibrium analyses under limit conditions. For example, the retaining structures for the basement excavation of the Fengcai-520 high-rise building are designed as depicted in Figure 4. The design utilizes H-shaped steel sections with dimensions H30 x 30 x 10 x 15, positioned with a center-to-center spacing of 80 centimeters between adjacent sections and a penetration depth of 33.8 meters.

Based on traditional design methodologies, the retaining structures for the Fengcai-520 high-rise basement excavation have been engineered according to the specified safety factors and equilibrium analyses, as illustrated in Figure 4. The design incorporates H-shaped steel sections (H30 x 30 x 10 x 15) with an 80-centimeter center-to-center distance between sections and a penetration depth of 33.8 meters.



(a) Schematic diagram of H-beam penetration depth into soil layers.



H30 x 30 x 1 x 1.5

(b) Center-to-center distance between two H-beams.

Figure 4. Retaining structures for the Fengcai-520 high-rise basement excavation using traditional design methods

Performance-Based Design

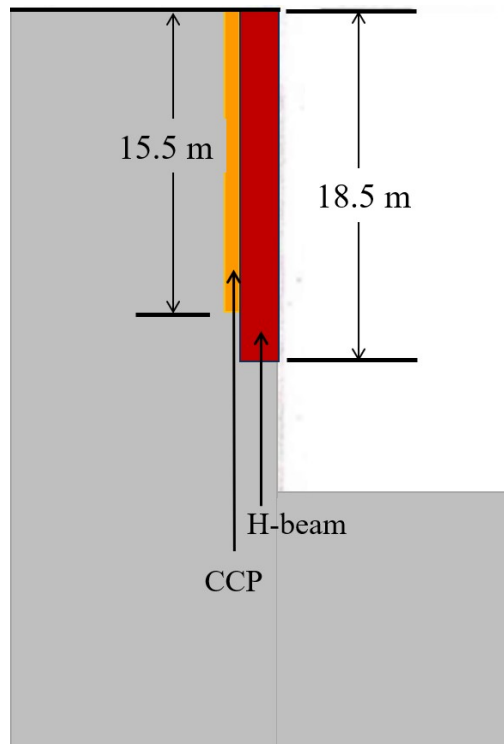
In performance-based design of retaining structures, traditional methods ensure that safety factors for resisting sliding, wall overturning, foundation bearing capacity, and overall stability are met under long-term loading and seismic forces. However, as illustrated in Figure 2, traditional retaining walls can still be prone to failure under

conditions such as heavy rainfall, earthquakes, or even calm, dry conditions.

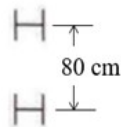
To address these limitations, experienced engineers can capitalize on the favorable geological conditions typical of Zhubei City, Taiwan. These conditions include dense silty gravel layers, sandstone, and mudstone interbeds with high shear strength and ver-

tical stability. By applying performance-based design principles and engineering judgment, more effective solutions can be achieved. For example, as shown in Figure 5, the design incorporates H-shaped steel sections (H30 x 30 x 10 x 15) with an 80-centimeter center-to-center spacing between adjacent sections and a penetration depth of

18.5 meters. Additionally, within a depth range of 15.5 meters, high-pressure jet grouting (CCP) is employed to inject a special cement slurry into the underground formation. This process rapidly consolidates the formation to create a strong, impermeable cut-off barrier, effectively reducing groundwater flow in shear bands.



(a) Schematic diagram of H-beam penetration depth and CCP operation depth.



H30 x 30 x 1 x 1.5

(b) Center-to-center distance between two H-beams.

Figure 5. Retaining structures for the Fengcai-520 high-rise basement excavation using performance-based design methods

In performance-based design, the primary objective is to ensure the overall safety of the Fongcai-520 high-rise building's basement upon completion. During the excavation of this basement, it is anticipated that sliding failure of the side walls may be inevitable, regardless of the depth to which the H-shaped steel sections are driven below the ground surface.

Given economic considerations, it is practical to permit some degree of sliding failure in the side walls within the performance-based design framework. This approach is analogous to the management of high, steep slopes in extensive mountainous highways or the side walls of long tunnel excavations. However, it is crucial that the area affected by sliding failure remains sufficiently small so that effective stabilization measures can be rapidly and efficiently implemented following a failure. Therefore, these stabilization measures must be pre-planned and integrated into the performance-based design.

Based on the performance-based design of the retaining structures illus-

trated in Figure 4, even if sliding failures occur in the side walls at various excavation stages or floors during the basement excavation of the Fongcai-520 high-rise building, the pre-planned stabilization strategies will ensure that the performance objectives for the excavation are met.

The Major Cause of Sliding Failures in the Basement Excavation of the Fongcai-520 High-Rise Building

Figure 6 depicts the finite element mesh of a plate subjected to continuous lateral compression. Figure 7 illustrates the deformation patterns that emerge when the strain in the plate enters the plastic range, resulting in localized deformations due to strain softening and the formation of shear bands within the finite element mesh. Figure 8 shows the contour map of excess pore water pressure within the groundwater underlying this plate. As indicated in Figure 7, shear banding during a seismic event leads to a highly concentrated excess pore water pressure within the shear bands.

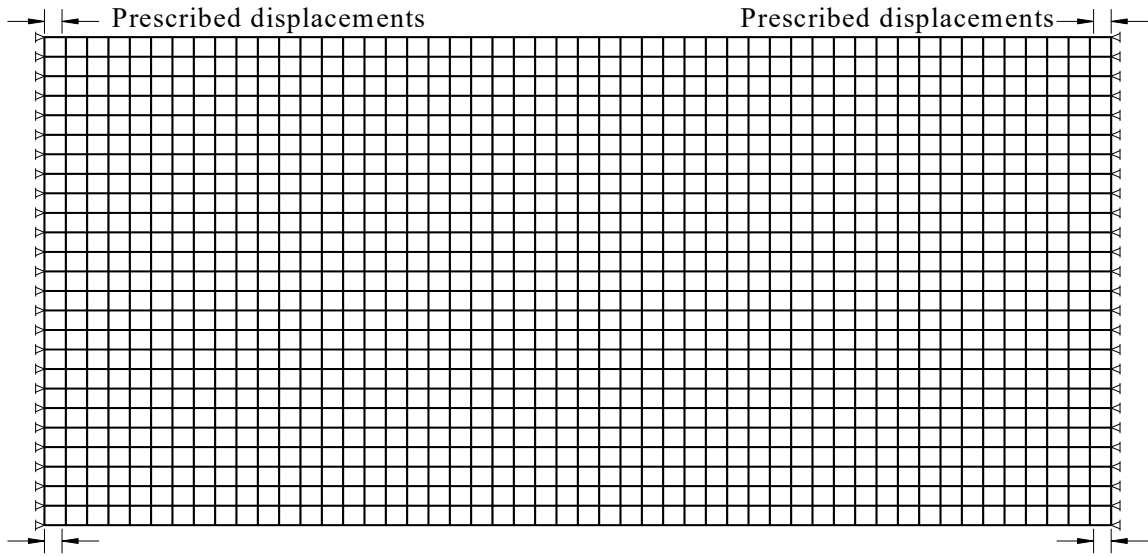


Figure 6. Finite element mesh, boundary conditions and prescribed lateral displacements (Hsu, 1987)

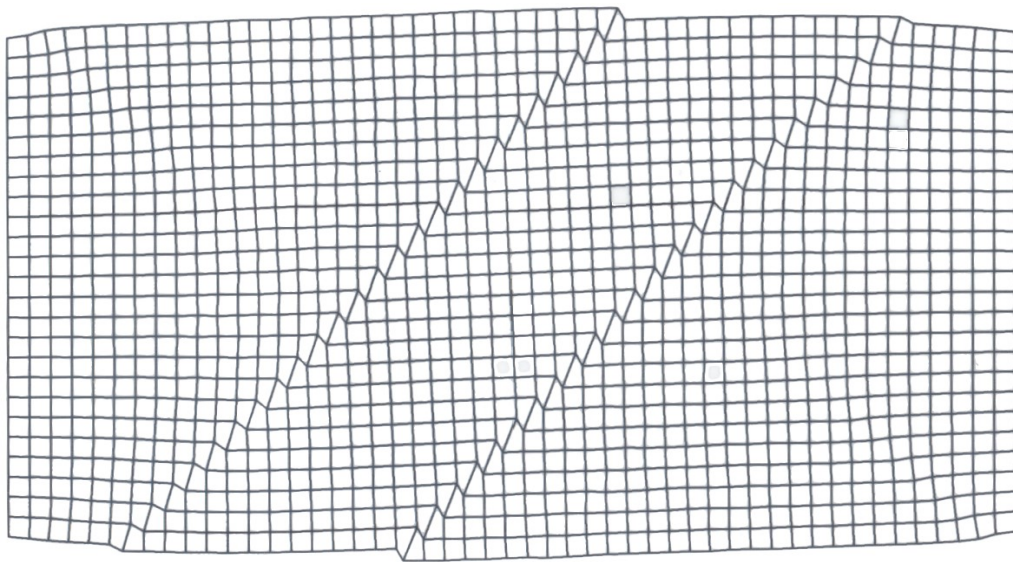


Figure 7. Deformed finite element mesh (Hsu, 1987)

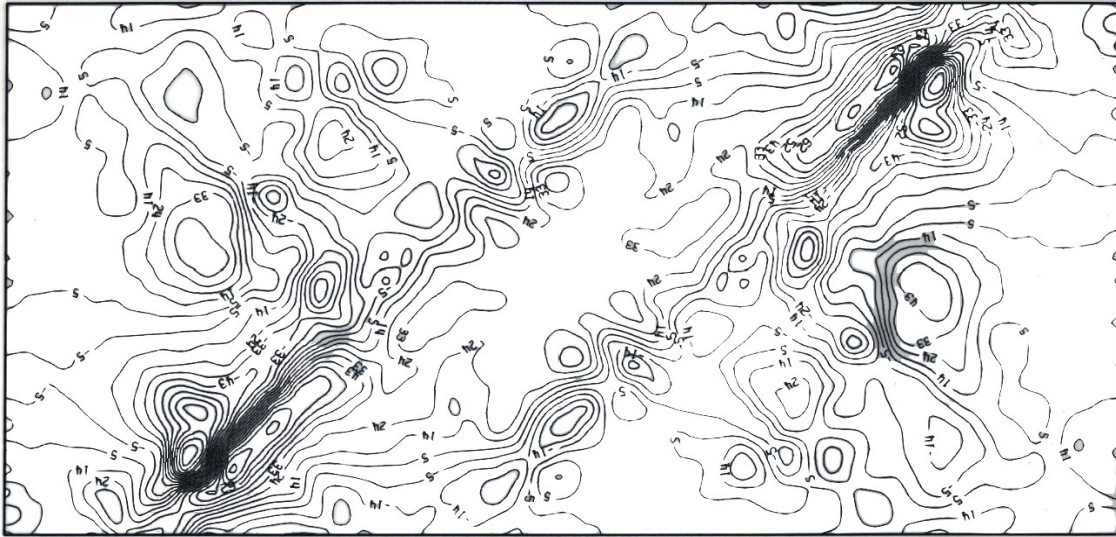


Figure 8. Contours of excess pore water pressures (Hsu, 1987)

Shear Bands and Shear Structures in the Fengcai-520 High-Rise Basement Side Wall

1. Figure 9 illustrates the shear textures within the total shear band width in the dense silty gravel layer

situated between two H-beams. The shear textures depicted include: principal displacement shear (D), thrust shear (P), Riedel shear (R), conjugate Riedel shear (R'), and compression texture (S).



(a) Before overlay.



(b) After overlay

Figure 9. Shear Bands and Shear Structures in the Dense Silty Gravel Layer Between Two H-Beams.

2. Figure 10 shows five distinct groups of shear textures within the total shear band width in the dense

silty gravel layer directly above the two H-shaped steel sections. These shear textures include: principal

displacement shear (D), thrust
shear (P), Riedel shear (R), conju-

gate Riedel shear (R'), and com-
pression texture (S).



(a) Before overlay.



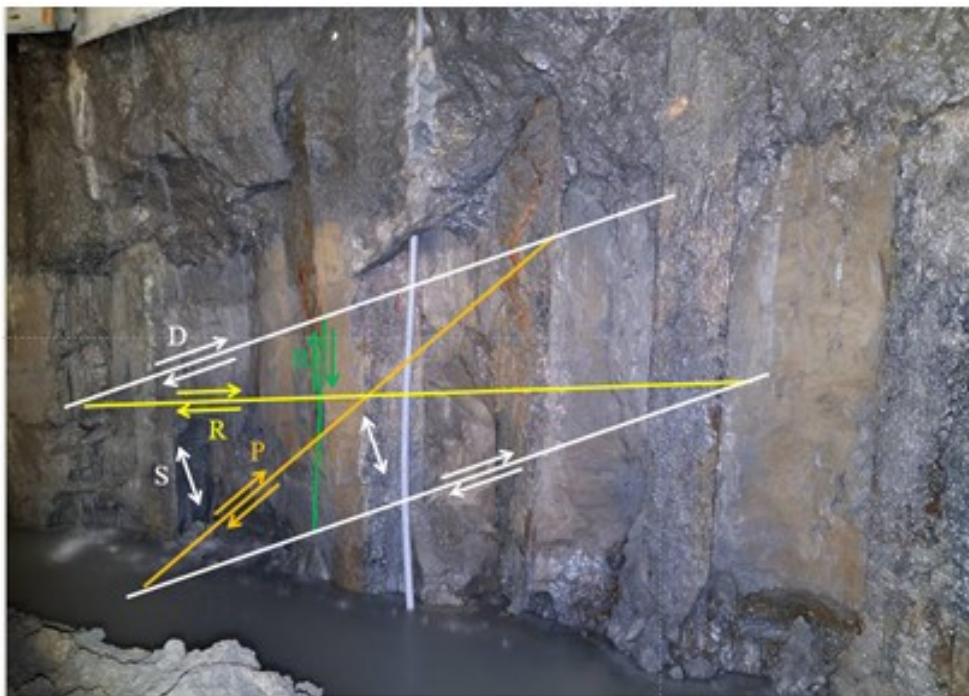
(b) After overlay.

Figure 10. Shear fracture zones and structures within the compact silty gravel layer directly above the rock strata between two H-beams.

3. Figure 11 displays five distinct groups of shear textures within the total shear band width of an interbedded mudstone and sandstone layer situated between two H-beams. The shear textures illustrated are: principal displacement shear (D), thrust shear (P), Riedel shear (R), conjugate Riedel shear (R'), and compression texture (S).



(a) Before overlay.



(b) After overlay.

Figure 11. Shear fracture zones and structures within an interbedded mudstone and sandstone layer between two H-beams.

4. Figure 12 illustrates five distinct groups of shear textures within the total shear band width of a second interbedded mudstone and sandstone layer situated between two H-

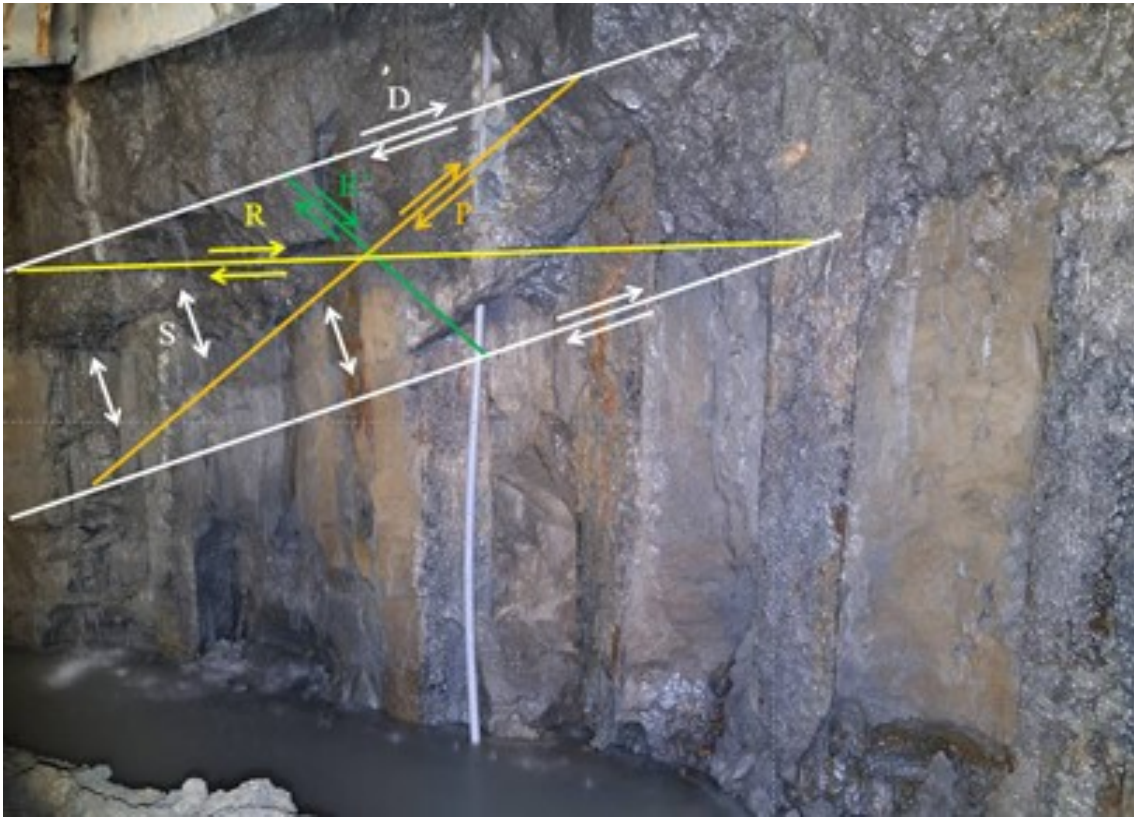
beams. The shear textures depicted are: principal displacement shear (D), thrust shear (P), Riedel shear (R), conjugate Riedel shear (R'), and compression texture (S).



(a) Before overlay.



(b) After overlay (1).



(c) After overlay (2).

Figure 12. Shear fracture zones and structures within a second interbedded mudstone and sandstone layer between two H-beams.

5. Figure 13 illustrates five distinct groups of shear textures within the total shear band width of the rock sidewall on the west side of underground level six. The shear textures shown include: principal displacement shear (D), thrust shear (P), Riedel shear (R), conjugate Riedel shear (R'), and compression texture (S).



(a) Before overlay.



(b) After overlay.

Figure 13. Shear fracture zones and structures within the rock sidewall on the west side of the underground level six.

Effectiveness of Stabilization Methods for Sliding Failures in the Basement Excavation of the Fongcai-520 High-Rise Building

During the excavation of the Fongcai-520 high-rise building's basement, a tectonic earthquake can induce shear banding effects that lead to highly concentrated excess pore water pressure within the groundwater along the shear bands. As shear banding accumulates, the rock within the shear band experiences increasing brittle fracturing. This fracturing produces rock debris that, once mobilized, are transported by groundwater through the interconnected pore spaces within the shear band. These debris can then

emerge through the shear band outcrops on the side walls of the basement, potentially causing sliding failures.

In the event of such sliding failures in the basement's side walls, on-site engineers can implement emergency response measures according to the strategies outlined in the performance-based design. The immediate response involves stabilizing the sliding failure by placing sandbags. Following this, high-pressure grouting operations, specifically using Cemented Column Pipe (CCP) techniques, are performed to construct a cut-off wall (refer to Figures 14(a) and 14(b)).



(a) Emergency stabilization of sliding with sandbags and water sealing with CCP (1).



(b) Emergency stabilization of sliding with sandbags and water sealing with CCP (2)

Figure 14. Performance design for emergency treatment of sliding failures on the basement sidewall.

Effectiveness of Stabilization Methods for Sliding Failures

Emergency stabilization measures, including the use of sandbags and Cemented Column Pipe (CCP) techniques, effectively addressed both the sliding failures and water ingress issues. Following the successful stabilization, construction of the reinforced concrete exterior walls commenced. Figure 15(a) shows the completed reinforced concrete exterior wall on the south side of

underground level six, while Figure 15(b) depicts the completed reinforced concrete exterior wall on the east side of the same level. These figures illustrate that, after resolving the localized sliding issues along the basement sidewalls, the construction of the reinforced concrete exterior walls for the underground levels could proceed as planned. The completion of these walls demonstrates that the performance design objectives were successfully achieved.



(a) Reinforced concrete exterior wall on the south side of the underground level six.



(b) Reinforced concrete exterior wall on the east side of the underground level six.

Figure 15. Completed reinforced concrete exterior walls on the south side and east side of the underground level six, after resolving sliding issues.

Comparison and Discussion

1. Figure 16 presents a schematic of the shear bands adjacent to the basement of the Fongcai-520 high-rise. These shear bands are influenced by shear banding effects typical of Zhubei City, Taiwan. As

tectonic plates undergo lateral compression, strain that progresses into the plastic range results in strain softening. This process induces localized deformations, leading to the formation of shear bands, as illustrated in Figure 6.

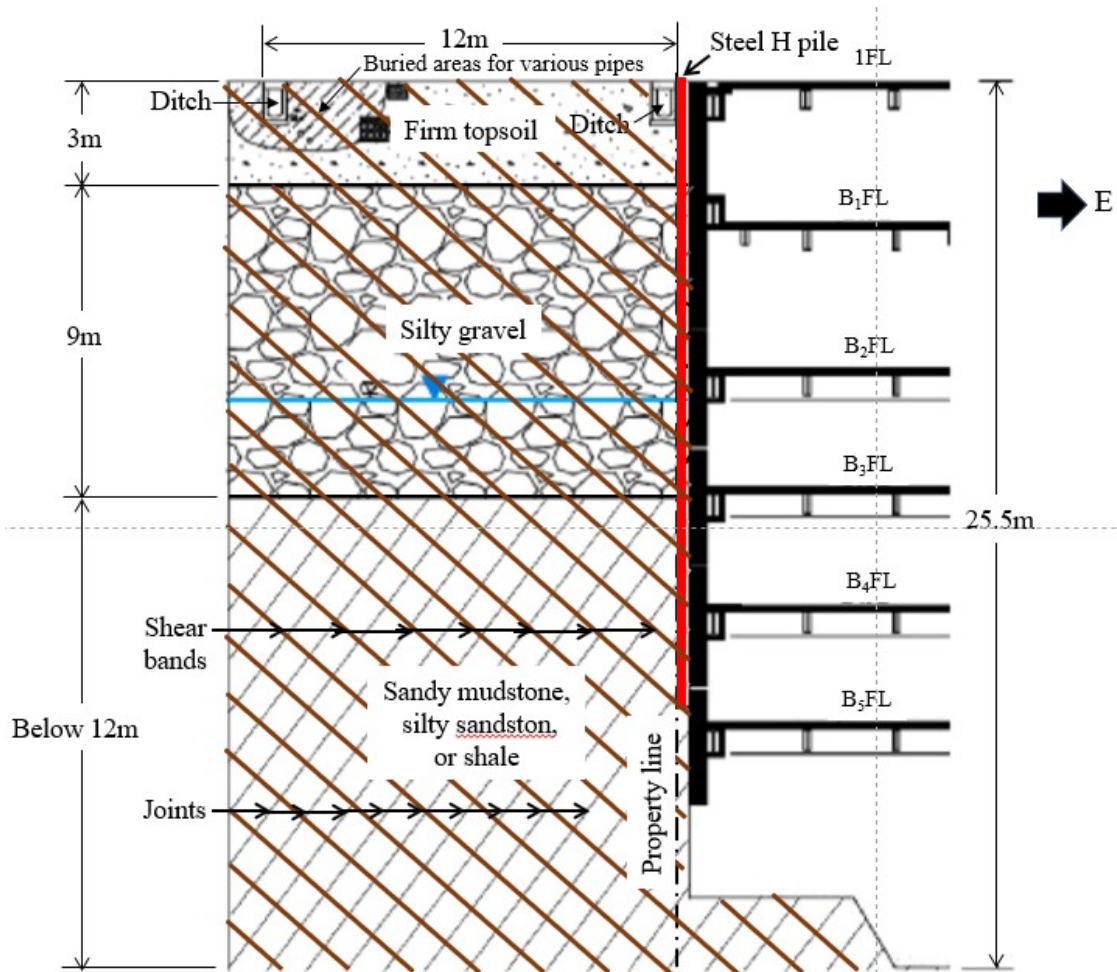


Figure 16. Schematic of shear bands adjacent to the basement of the Fengcai-520 high-rise.

2. Figure 17 illustrates the shear bands that develop within a tectonic plate during tectonic earthquakes. During shear banding, the phenomenon of slip-stick behavior occurs due to frictional resistance, as depicted in Figure 18. In this process, slip causes the plate to accelerate, while stick results in de-

celeration. This repeated slip-stick behavior leads to fluctuations between acceleration and deceleration. Consequently, during repeated tectonic earthquakes, shear banding is associated with acceleration-time curves of ground vibrations, as shown in Figure 19. .



Figure 17. Shear bands observed in Zhushan, Taiwan during the 921 Ji-Ji earthquake (Hsu, 2022)

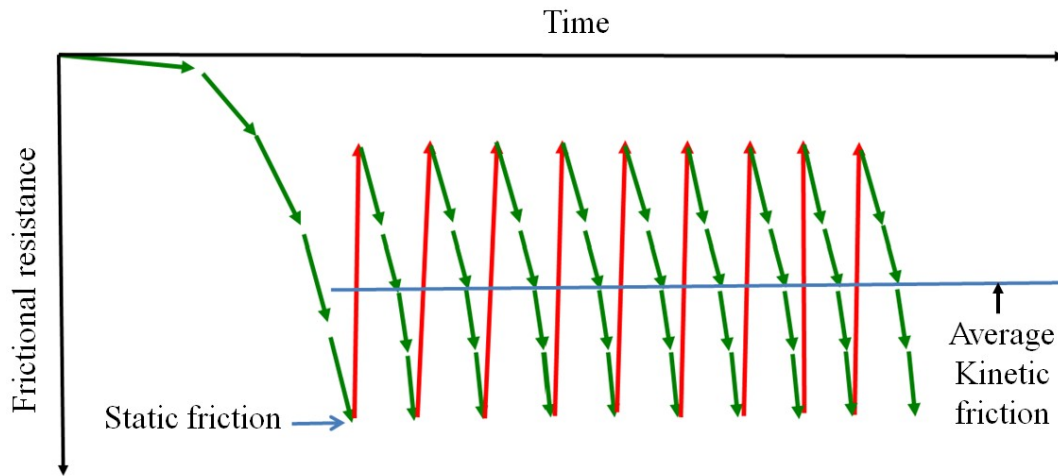


Figure 18. Stick-slip phenomenon in shear bandings
(redrawn from Lambe and Whitman (1969))

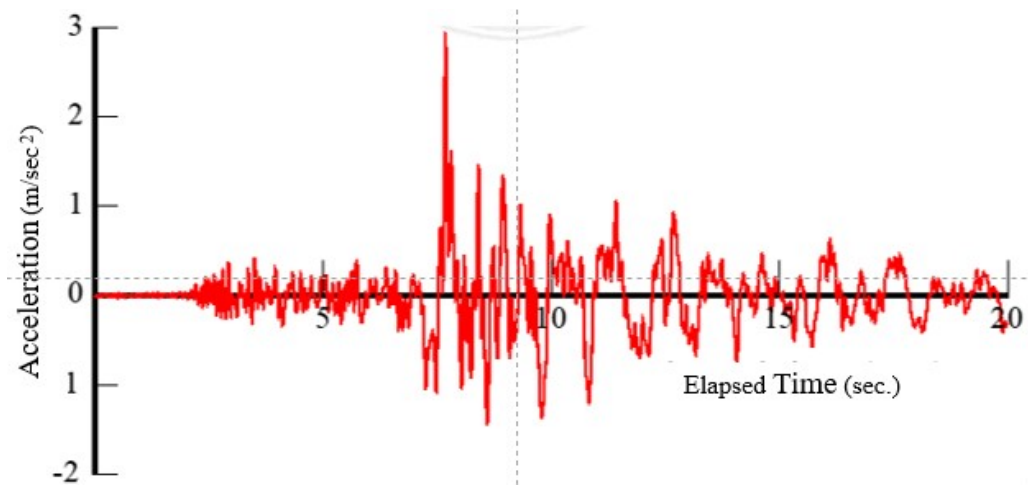


Figure 19. Ground acceleration time-history curve of the seismometer record

3. When shear band rocks fracture into debris and there is a high concentration of excess pore water pressure within the groundwater along the shear band, the rock debris will become buoyant and be transported by the groundwater. This debris will eventually emerge through the shear band outcrops, as illustrated in Figure 20.
4. For the Fongcai-520 high-rise building's basement, although the traditional design specifies a penetration depth of up to 33.8 meters

for the H-shaped steel supports, with an 80 cm center-to-center spacing between the supports, the presence of shear bands in the adjacent silty gravel layer and mudstone and sandstone interlayers (see Figure 16) indicates that neither a penetration depth of 33.8 meters

nor 18.5 meters below the surface is sufficient to prevent the development of shear banding effects in these layers. As a result, sliding failure issues are likely to occur in the basement sidewalls of the Fongcai-520 high-rise building, as shown in Figure 21.



Figure 21. Sliding failure of rock debris from shear bands observed in the side walls of the Fongcai-520 high-rise building's basement.

5. Comparison of emergency response plans for traditional design and performance-based design

When both conventional and performance-based designs anticipate potential sliding failure issues during basement excavation, reliance solely on traditional design

methods can be problematic. Traditional approaches often assume that meeting regulatory safety factors for retaining structures guarantees the prevention of sliding failures during excavation. This assumption can lead to a lack of emergency response plans to address such failures.

In contrast, performance-based design acknowledges that no matter how deeply H-beams are embedded, shear banding effects cannot be entirely eliminated. Therefore, for the excavation of the Fongcai-520 high-rise basement, performance-based design anticipates sliding failures due to shear banding and includes pre-planned emergency response strategies specifically to address these issues.

6. Comparison of Emergency Response Effectiveness Between Traditional and Performance-Based Design

In traditional design practices, the absence of an emergency response plan means that immediate remedial measures cannot be implemented when sliding failures occur during basement excavation. If these sliding problems are not addressed promptly, several adverse outcomes may arise: (1) delays in remediation, (2) impacts on construction progress, and (3) risks to structural safety. Consequently, without timely intervention, the subsequent construction of the reinforced concrete sidewalls in the basement and the overall structural integrity of the Fongcai-520 high-rise may be compromised. Thus, traditional design approaches, lacking an emergency response plan, risk significant negative impacts on both the construction process and the structural safety of the completed basement.

In contrast, performance-based design incorporates emergency response measures. If sliding failures occur during basement excavation, these pre-planned measures can be immediately implemented to address the issues swiftly. As a result, high excess pore water pressures in the groundwater within the shear bands, induced by tectonic earthquakes, will rapidly decrease. This effective resolution of sliding issues prevents further disruption to the construction of the reinforced concrete sidewalls and ensures the overall structural safety of the Fongcai-520 high-rise basement upon completion, thereby clearly achieving the performance design objectives.

Conclusions and Recommendations

The geological strata in Zhubei, Taiwan, primarily consist of densely packed silty gravel layers, sandstone, and shale interlayers. These layers generally exhibit high shear strength and vertical stability, which typically reduces the likelihood of sliding failures in basement walls during excavation. Despite these favorable conditions, the Fengcai-520 high-rise basement excavation has encountered persistent sliding failures. Experts and scholars have often attributed these issues to deviations from traditional design practices. To elucidate the primary causes of these persistent failures, this paper uses the Fengcai-520 high-rise basement excavation in Zhubei as a case study and presents the following conclusions based on comparative analysis and

discussion:

1. Occurrence of Sliding Failures: Both traditional and performance-based designs are susceptible to sliding failures during the excavation of the Fengcai-520 high-rise basement. This issue is persistent regardless of the design approach employed.
2. Impact of Tectonic Activity: Taiwan's high seismic activity leads to continuous shear displacements along fault zones, increasing the brittleness of the fault zone rocks. During fault displacements, excess pore water pressure in the groundwater within the fault zones can become highly concentrated locally. Consequently, rock debris from the fault zone, buoyed by groundwater, may flow into the basement.
3. Effectiveness of Performance-Based Design: Performance-based design is uniquely effective in addressing and mitigating sliding failures of basement walls. It also resolves the issue of highly concentrated excess pore water pressure in fault zone groundwater, preventing further complications during subsequent excavation activities. This approach ensures the structural safety of the basement upon completion.

Based on these conclusions, the authors recommend adopting performance-based design methods for future basement excavations. This approach balances economic feasibility with the need for controlled management of sliding failures. By swiftly addressing and resolving these issues, performance-based design ensures the struc-

tural integrity of the completed basement and achieves the performance design goals.

References

- National Land Management Agency, Ministry of the Interior, *Buinding Foundation Design Code*, 2023
- Chen, Wai-Fah, *Limit Analysis and Soil Plasticity*, Elsevier Scientific Pub. Co.: Amsterdam, The Netherlands; New York, NY, USA, 1975
- Google, Google Earth, Website: <https://earth.google.com/>, 24
- Hsu, Tse-Shan, *Capturing Localizations in Geotechnical Failures*, Ph.D. Dissertation, Civil Engineering in the school of Advanced Studies of Illinois Institute of Technology , 1987.
- Hsu, Tse-Shan, "The Major Cause of Earthquake Disasters: Shear Bandings," A Chapter in "Earthquakes-Forecast, Prognosis and Earthquake Resistant Construction," Edited by Valentina Svalova, IntechOpen, pp. 31-48, 2018
- Hsu, Tse-Shan, Yi-Ju Chen, Zong-Lin Wu, Yi-Lang Hsieh, Jiann-Cherng Yang, Yi-Min Huang, "Influence of Strain Softening and Shear-band Tilting Effect on the Maximum Earth Pressure of Retaining Walls," *International Journal of Organizational Innovation*, Vol. 14, No. 1, pp. 45-86, Website:

<https://www.ijoi-online.org/attachments/article/328/1167%20final.pdf>, 2021

Lambe, T. William and Whitman, Robert V., *Soil Mechanics*, John Wiley & Sons, New York, pp. 65, 1969.

Mechanics and Foundations, Basic Geotechnics, 5th Edition, Pearson, Prentice Hall, 2007

Simonelh, A. L. and Penna, A., Performance-Based Design of

Gravity Retaining Walls Under Seismic Actions. Edited by Cosenza, E., Eurocode 8 Perspectives from the Italian Standpoint Workshop, Napoli, Itali, pp. 277-289, Website: <http://www.geoplanning.it/test/wp-content/uploads/2012/02/Performance-based-design-of-gravity-retaining-walls-under-seismic-actions-.pdf> , 2009